ARCHIVES OF ACOUSTICS
8, 3, 205-222 (1983)

DETECTABILITY OF CALCIFICATIONS IN BREAST TISSUES BY THE ULTRASONIC ECHO METHOD

LESZEK FILIPCZYŃSKI

Department of Ultrasound, Institute of Fundamental Technological Research, Polish Academy of Sciences (00-049 Warsaw, ul. Świętokrzyska 21)

The tumour processes in breasts involve calcifications which can be detected using ultrasonic methods. The aim of the present paper is to determine the minimum size of these calcifications which can be detected by the ultrasonic echo method.

The models of the calcification which was assumed in this paper are a rigid and an elastic sphere onto which a plane wave is incident. Such density and longitudinal wave velocity were assumed here as are characteristic of the skull bone, and it is for these values that the far field form function $f_\infty(ka)$ was determined for different values of the Poisson's ratio.

On the basis of these calcification models, the detectability of the calcification by the echo method was evaluated, showing that, when a typical ultrasonograph at a frequency of 3 MHz is used, sphere-shaped calcifications with radii from 4 μm to 52 μm, depending on the depth at which they occur, give signals at the level of the electronic noise of the ultrasonograph.

Experimental research has shown that the detectability by the echo method is restricted by breast tissue heterogeneities which cause the interfering background to occur. The level of these interference signals was determined at a frequency of 3 MHz. At 4 cm depth this level was higher by 31 dB than the electronic noise level. From these results, the present author determined the radii of calcifications detectable by the echo method at a level higher by 20 dB (ten times higher) than the level of the tissue interference signal. The radii are 0.05, 0.15 and 1 mm long at the respective depths of 2, 4 and 6 cm. Their dependence on the depth results mainly from the wave attenuation in tissues, which increases as the depth at which a given calcification is, grows. A linear receiver should be used for calcification detection.

Notation

A — attenuation loss on the path of the wave
a — radius of the sphere
c — wave velocity in soft tissue

c_m — expansion coefficients
m — natural number
c_L — longitudinal wave velocity in the calcification
c_T — transverse wave velocity in the calcification
c — wave velocity in the medium which constitutes the tissue reflector
D — level increase caused by tissue interference (Fig. 10)
$f_\infty(ka)$ — far field form function
$h^{(2)}$ — spherical Hankel function of the second kind
$h^{(2)'}$ — derivative of the function $h^{(2)}$ with respect to the argument
j — $\sqrt{-1}$
j_m — spherical Bessel function
j_m', j_m'' — derivatives of the function j_m with respect to the argument
$k = \omega/c$ — wave number
n_m — spherical Neumann function
n_m' — derivative of the function n_m with respect to the argument
N — electronic noise level
P_m — Legendre polynomial
p_i — pressure of the plane wave incident on the sphere
p_0 — pressure amplitude of the plane wave
p_s — pressure of the wave scattered by the sphere
p_{s0} — pressure amplitude of the wave scattered by the sphere
R — depth at which the calcification occurs
r — radial component of the polar coordinate system
T — double electroacoustic transducing loss
t — time
U_r — electric sensitivity of the ultrasonograph receiver
U_t — output voltage of the ultrasonograph transmitter in a pulse
W — electric dynamics of the ultrasonograph
x, x_1, x_2 — auxiliary quantities (see formulae (12a b, c))
α — pressure attenuation coefficient
η_m — phase angle of partial spherical waves reflected
θ — angular coordinate of the polar coordinate system
ν — Poisson's ratio
ϱ — density of the tissue medium
ϱ_s — density of the sphere
ϱ' — density of the tissue reflector
φ_m — auxiliary quantity (see formula (11))
ω — angular frequency

1. Introduction

The ultrasonic method is one of the more recent ways of detecting breast tumours [14]. Despite the intensive research performed on it in a large number of scientific centres, the possibilities of the ultrasonic diagnosis of breast tumours are far from exhausted. One example of the developments in this field is the Doppler ultrasonic methods which permit the observation of changes in the blood supply to the tumour when it is malignant [15].

Another problem in the diagnosis of breast tumours is the detection of calcifications by the ultrasonic echo method. The reactions which proceed in breast tissue cells and which cause calcifications when the cancer occurs are present in a very early stage of its development. They usually occur prior to the infiltrative phase, which is visible in a mammogram or an X-ray microgram preparation [16].

The detection of the microcalcifications is therefore fundamentally significant in the early diagnosis of breast tumours. In view of this, the question arises as to what are the possibilities of detecting small calcifications by the ultrasonic method.

The recent papers on the problems in ultrasonic investigations of the breast report on microcalcifications being detected only by mammographic methods; they cannot be detected, however, by ultrasound [21].

This paper presents an attempt to explain this problem and to determine the minimum calcification size which can be detected by ultrasonic echo method.

2. Assumptions of the analysis

Fig. 1 shows the ultrasonic system used here for detecting calcifications by the echo method. The first stage of these considerations consists in an evaluation of the magnitude of the ultrasonic wave reflected from a sphere-shaped calcification with a radius a.

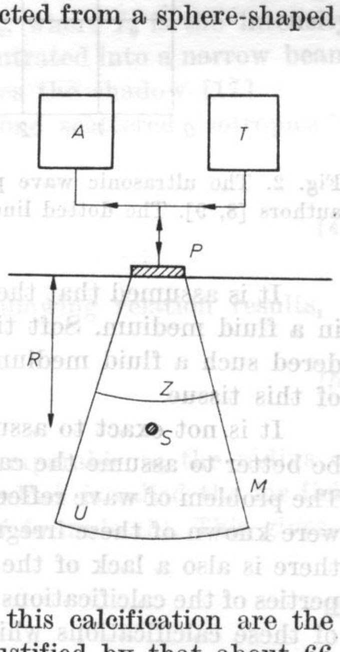

Fig. 1. The ultrasonographic system used in the investigations. T — transmitter, A — receiver, P — piezoelectric transducer swinging over an angle of 30°, M — medium investigated, S — calcification, U — area of the medium covered by the ultrasonic beam, Z — electronic distance indicator, R — depth at which the calcification occurs

It is assumed that the acoustic parameters of this calcification are the same as those of bone tissue. This assumption is justified by that about 66 per cent of the bone mass consists of inorganic matter, including mainly calcium salts [19]. The acoustic properties of bone tissue have been investigated by a large number of authors, who have obtained a rather considerable scatter of the measured values. Fig. 2 shows the results of ultrasonic wave velocity measurements, drawn from the available literature [8, 9]. The present considerations are based on the results of the measurements of WHITE *et al.* [23], who, working on rather ample experimental material, obtained the following data for the skull bones: the longitudinal wave velocity $c_L = 3.2$ km/s, the density $\varrho = 2.23$ g/cm³, the specific acoustic impedance $c_L = 7.1 \times 10^5$ g cm^{-2} s^{-1}. Neither these authors nor any other have given data on the transverse wave velocity.

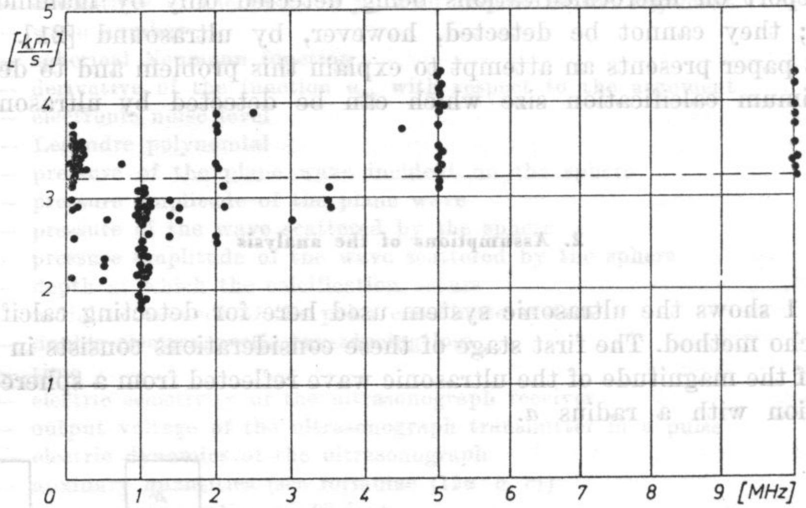

Fig. 2. The ultrasonic wave propagation velocity in bone tissue, measured by different authors [8, 9]. The dotted line indicates the value assumed in the present considerations

It is assumed that the calcification has the shape of a sphere and is placed in a fluid medium. Soft tissue can with rather good approximation be considered such a fluid medium and water, in turn, can be a good approximation of this tissue.

It is not exact to assume that the calcification is sphere-shaped. It would be better to assume the calcification as a solid with irregularly shaped surface. The problem of wave reflection from such a solid could be solved if the statistics were known of these irregularities [24]. These data are not available, however, there is also a lack of the simpler information on the density, the elastic properties of the calcifications etc. There is also no information on the heterogeneity of these calcifications which occur in the breast.

In view of this, the present problem must be considered with approximation, by assuming two calcification models: in the form of an ideal rigid sphere and an ideal elastic one. The analysis will be performed for steady-state (continuous wave).

3. Ultrasonic wave reflection from a rigid sphere

The acoustic pressure of a plane wave incident in a fluid onto the sphere can be represented, in a polar coordinate system whose centre coincides with the centre of the sphere, in the form of the infinite series [20, 17]

$$p_i = p_0 \exp(j\omega t + kr\cos\theta) = p_0 \exp(j\omega t) \sum_{m=0} j^m (2m+1) P_m(\cos\theta) j_m(kr). \quad (1)$$

The acoustic pressure of the wave scattered by the sphere is in the form

$$p_s = \sum_{m=0}^{\infty} c_m P_m(\cos\theta) h_m^{(2)}(kr) \exp(j\omega t), \quad (2)$$

where the expansion coefficients c_m are determined from the boundary conditions on the surface of the sphere. When the sphere is rigid and immovable, these coefficients take the form

$$c_m = j^m (2m+1) \frac{j'_m(ka)}{h_m^{(2)}(ka)}. \quad (3)$$

When the wavelength is very short with respect to the radius of the rigid sphere, the power scattered by the sphere is $\pi a^2 I_0$, where I_0 is the intensity of the incident plane wave; the same power is concentrated into a narrow beam which interferes with the primary beam and causes the shadow [17].

Comparison of the incident power with the one scattered isotropically by the sphere gives the equation

$$\frac{\pi a^2 p_0^2}{2\varrho c} = \frac{4\pi r^2 p_{s0}^2}{2\varrho c}, \quad (4)$$

where the distance $r \gg a$. Hence, directly the following relation results,

$$p_{s0} = p_0 \frac{a}{2r}. \quad (5)$$

In a general case, when the wavelength is comparable to the radius of the sphere or longer, the additional factor $f_\infty(ka)$, which is called the far field form function, is introduced into the right side of formula (5). This gives

$$p_{s0} = p_0 \frac{a}{2r} f_\infty(ka). \quad (6)$$

For the rigid sphere the function $f_\infty(ka)$ takes the form of the curve S shown in Fig. 3 [13]. The undulations in the curve result from the wave interference around the sphere, since, in view of its ideal rigidity, the wave does not penetrate inside. In real calcifications, whose surface is irregular and whose shape is only similar to a sphere, the curve is not so regular as in Fig. 3.

The previous considerations were concerned with an immovable sphere. When affected by the incident wave, the sphere can move freely. This problem was investigated by HICKLING and WANG [13], who showed that a rigid sphere

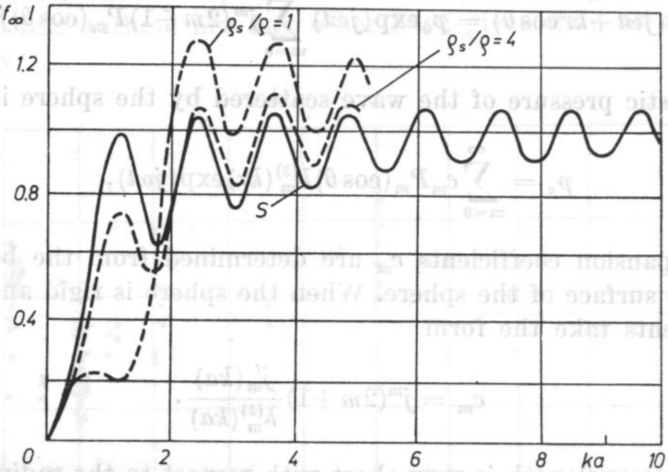

Fig. 3. The function $f_\infty(ka)$ for a rigid sphere in a fluid, according to HICKLING and WANG [13]

vibrates when acoustic pressure acts on it. In view of this, the form of the function $f_\infty(ka)$ changes, particularly over the range $ka < 5$. The magnitude of this change depends on the density of the sphere and on the density of the surrounding medium. Fig. 3 shows curves calculated by HICKLING and WANG for the ratios $\varrho_s/\varrho = 1$ and 4.

For the calcifications of interest here, whose density is about twice as large as that of the surrounding tissue, the real curve of $f_\infty(ka)$ should be close to both curves in Fig. 3.

4. Ultrasonic wave reflection from an elastic sphere

In the case of an ideal elastic sphere the problem of reflection becomes more complex [2, 3, 12, 18]. In addition to reflected waves, longitudinal and transverse waves penetrate inside the sphere. The latter waves arise at the interface of the fluid medium and the sphere. The expansion coefficients (2) take then the form

$$c_m = -p_0(-j)^{m+1}(2m+1)\sin\eta_m \exp(j\eta_m). \tag{7}$$

The angle η_m is a function of the velocity of longitudinal and transverse waves within the sphere and of longitudinal waves in the surrounding medium, and of the radius of the sphere and frequency. The way of determining the angles η_m was given in paper [3] and subsequently verified in papers [12, 22].

With backscattering ($\theta = 180°$) the Legendre polynomials disappear from expression (2), since $P_m(-1) = (-1)^m$. For long distances a spherical Hankel function can be represented by the asymptotic expression [20]

$$h_m^{(2)}(kr) = \frac{1}{kr}\exp\left[-j\left(kr - \frac{m+1}{2}\pi\right)\right]. \tag{8}$$

Thus, when coefficients (7) are taken into account and the time factor neglected, formula (2) becomes [18]

$$p_s = p_0\frac{a}{2r}\left[\frac{-2}{ka}\sum_{m=0}^{\infty}(2m+1)(-1)^m \sin\eta_m \exp(j\eta_m)\right] = p_0\frac{a}{2r}f_\infty(ka), \tag{9}$$

where

$$\tan\eta_m = -\frac{j_m(x)}{n_m(x)}\left[\tan\varphi_m - x\frac{j_m'(x)}{j_m(x)}\right]\left[\tan\varphi_m - x\frac{n_m'(x)}{n_m(x)}\right]^{-1} \tag{10}$$

and

$$\tan\varphi_m = \frac{\varrho}{\varrho_s}\left[\frac{x_2^2}{2}\frac{\dfrac{x_1 j_m'(x_1)}{x_1 j_m'(x_1) - j_m(x_1)} - \dfrac{2(m^2+m)j_m(x_2)}{(m^2+m-2)j_m(x_2) + x_2^2 j_m''(x_2)}}{\dfrac{x_1^2\{[\nu/(1-2\nu)]j_m(x_1) - j_m''(x_1)\}}{x_1 j_m'(x_1) - j_m(x_1)} - \dfrac{2(m^2+m)[j_m(x_2) - x_2 j_m'(x_2)]}{(m^2+m-2)j_m(x_2) + x_2^2 j_m''(x_2)}}\right]. \tag{11}$$

Expressions (10) and (11) include the quantities

$$x = ka = \frac{\omega}{c}a,\; x_1 = k_1 a = \frac{\omega}{c_L}a,\; x_2 = k_2 a = \frac{\omega}{c_T}a \tag{12a,b,c}$$

and the Poisson's ratio ν which is related to the velocity of longitudinal and transverse waves by the relation

$$c_T = c_L\sqrt{\frac{1-2\nu}{2(1-\nu)}}. \tag{13}$$

Fig. 4 gives the values of the Poisson's ratio for different materials, depending on the ratio of the transverse wave velocity to the longitudinal wave velocity. This ratio increases as the material becomes in terms of elasticity increasingly similar to a fluid, for which it reaches the value $\nu = 0.5$. In view of their elastic properties, it seems that calcifications should be assigned to the group of materials close to glass, porcelain or molten quartz, for which the Poisson's ratio ν varies between 0.17-0.26.

Taking as the basis the theory of wave reflection from an ideal elastic sphere, from formulae (9), (10) and (11), the far field form function $f_\infty(ka)$ was determined for the parameters of calcifications given in point 3, with different values of the Poisson's ratio $\nu = 0$; 0.1; 0.2; 0.3 and 0.4. These calculations were carried out on a Cyber 70 (IBM) computer and their results are shown in Figs. 5 and 6. It follows from the curves obtained that a distinct effect of

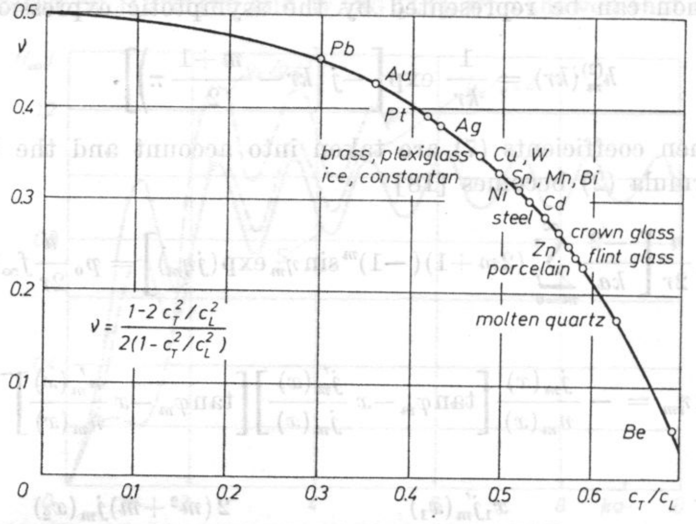

Fig. 4. The Poisson's ratio ν for different materials, depending on the ratio of the transverse wave velocity c_T to the longitudinal wave velocity c_L

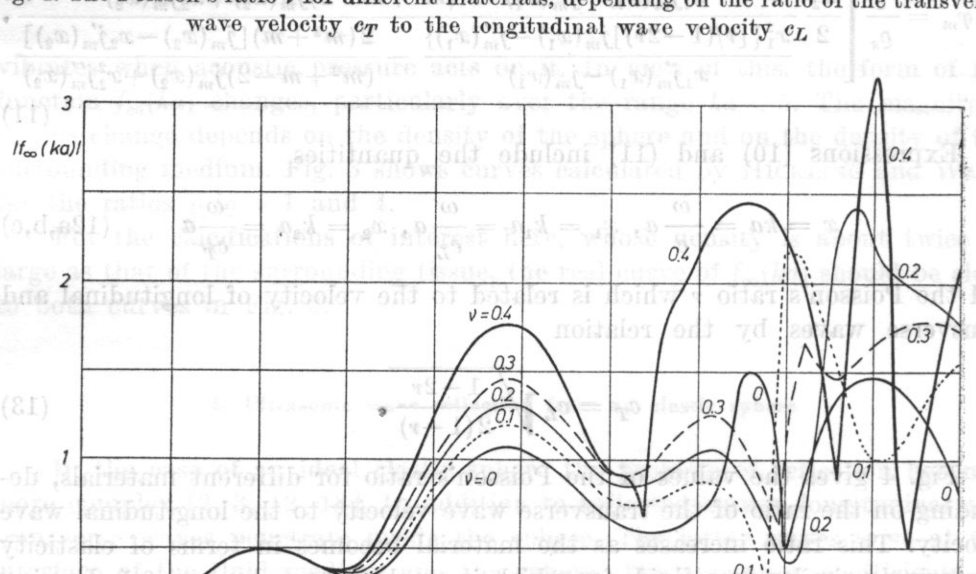

Fig. 5. The function $f_\infty(ka)$ of the sphere (in the calcification for $c_L = 3.2$ km/s, $\varrho_s = 2.23$ g/cm³, in the tissue for $c_L = 1.5$ km/s, $\varrho = 1$ g/cm³) determined for various values of the Poisson's ratio ν

the Poisson's ratio on the behaviour of the function $f_\infty(ka)$ does not occur until the value $ka > 1.5$.

It is interesting to note that the existing theories of wave scattering by elastic spheres apply to immovable spheres. It should not be excluded that, as for rigid spheres, the phenomenon of scattering will behave in a slightly

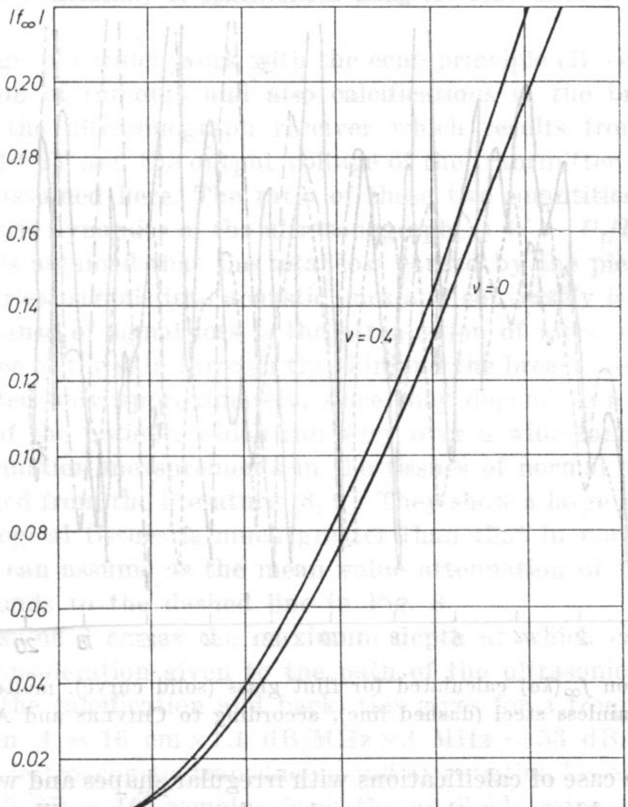

Fig. 6. The function $f_\infty(ka)$ of the sphere as in Fig. 5 but for small arguments of ka

different way, when the possibility of spheres being movable under the effect of pressures acting on their surfaces is taken into account.

Fig. 7 shows the functions $f_\infty(ka)$ calculated for flint glass, molten silica and stainless steel by CHIVERS and ANSON [1], which all show similar behaviour. Their maxima and minima result from the interference of waves around the sphere and also from resonances within it.

In their investigations of the scattering phenomenon, FLAX *et al.* [7] used a formalism drawn from nuclear reaction theory. They showed that in the case of bodies with density and wave velocities greater than those of the surrounding fluid, scattering is a result of the superposition of the phenomenon of wave scattering by a rigid body and a number of resonances which occur in these bodies. These resonances differ in character, since they correspond to different wave types, including, for example, also surface waves and waves of the "whispering gallery" type.

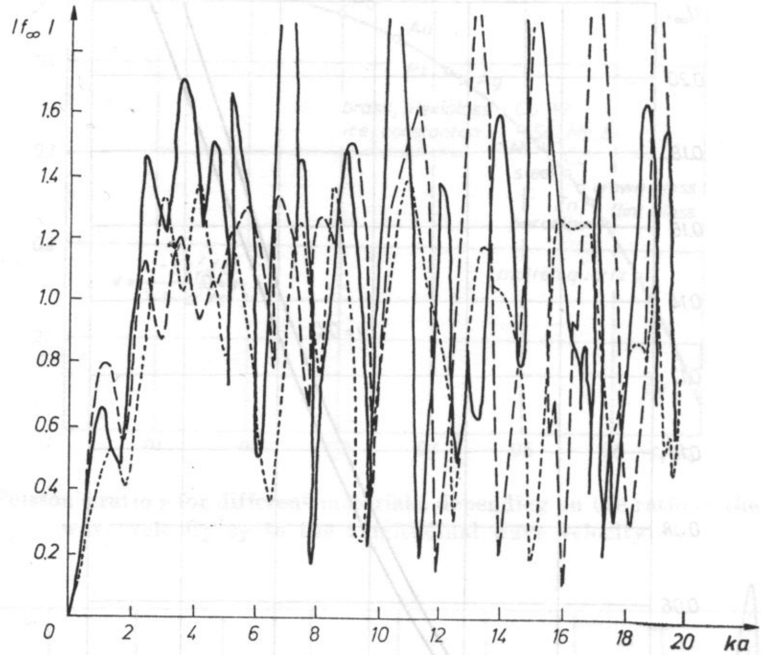

Fig. 7. The function $f_\infty(ka)$ calculated for flint glass (solid curve), molten silica (dotted line) and stainless steel (dashed line), according to CHIVERS and ANSON [1]

Thus, in the case of calcifications with irregular shapes and with corrugated surfaces, one should expect that a number of resonances will not occur at all and the curve of the function $f_\infty(ka)$ will come closer to the curve of a rigid body. From Fig. 7, it can thus be assumed that the maxima and minima will smooth out about the mean value, which for $ka > 3$ can be taken as $f_\infty(ka) = 1$. A similar conclusion can be drawn for rigid spheres (Fig. 3).

Extensive experimental investigations of the scattering of acoustic waves by metal (aluminium and brass) spheres submerged in water were carried out by HAMTON and MCKINEY [11] over the range 4.1 – 57 of the product ka. They showed that for large values of ka, backscattering is constant as a function of scattering and slightly less than follows from theoretical data for a rigid sphere. The present assumption of the constant value of the function $f_\infty(ka)$ was thus confirmed experimentally. It is, however, necessary to note that the conclusion formulated above for large values of ka only applies to the amplitudes of pulses reflected from the surface of the sphere and is not valid for those which arise as a result of multiple reflection within the sphere. This condition corresponds to a lack of resonances, i.e. such a situation which is expected with calcification of irregular shape and unsumooth surface.

5. Detectability of calcifications using the echo method

Ultrasonographs which work with the echo principle (B — mode) are used in the detection of tumours and also calcifications in the breast. A typical sensitivity of the ultrasonograph receiver which results from its electronic noise is $U_r = 10\ \mu V$ and the output voltage of the transmitter in a pulse $U_t = 250$ V are assumed here. The ratio of these two quantities, which will be called the electric dynamics of the ultrasonograph, is $W = U_t/U_r = 2.5\times10^7 = 148$ dB. It is assumed that the total loss caused by the piezoelectric transducing of electrical signals into acoustic ones and conversely is $T = 15$ dB [5].

Another cause of signal loss is the attenuation of ultrasound on its path from the surface of the skin through the skin and the breast tissue. These losses can be evaluated only approximately, since they depend to a large extent on the anatomy of the patient, which can vary over a wide range. Fig. 8 shows values of attenuation measurements in the tissues of normal and pathological breasts, collected from the literature [8, 9]. They show a large scatter; attenuation in pathological tissues is much greater than that in normal tissues. For the latter one can assume as the mean value attenuation of 1.1 dB/MHz cm, which corresponds to the dashed line in Fig. 8.

Let us assume 8 cm as the maximum depth at which calcifications can occur. With consideration given to the path of the ultrasonic wave from the transducer to the calcification and back, this gives for a frequency of 3 MHz the attenuation $A = 16\ \mathrm{cm}\times1.1\ \mathrm{dB/MHz}\times3\ \mathrm{MHz} = 53$ dB.

After the electroacoustic transducing and attenuation losses are subtracted, $W-T-A = 80\ \mathrm{dB} \doteq 10^4$ remains from the available range of the electrical dynamics W of the ultrasonograph. The ratio of the pressure amplitude of the wave reflected from the calcification at the distance $R = 8$ cm to the pressure amplitude of the wave incident on the calcification should be higher than a value of 10^{-4}. Only than the electrical signal detected by the ultrasonograph will be greater than the electronic noise level of the receiver.

When a rigid, immovable sphere is assumed as the calcification model, for $ka < 1$ it is possible to write, according to RSHEVKIN [20],

$$p_s = -p_0\frac{(ka)^3}{3kr}\left(1+\frac{3}{2}\cos\theta\right)\exp[j(\omega t-kr)]. \tag{14}$$

Hence, in the case of backscattering when $\theta = 0$ (Rshevkin [20]), unlike the papers cited above [3, 12, 22], the opposite incidence direction of the wave is assumed here; hence, the angle $\theta = 0$ and not 180°, and neglecting the phase factor, for $ka < 1$,

$$\frac{p_s}{p_0} = \frac{5}{6}\frac{(ka)^3}{kr} > 10^{-4}. \tag{15}$$

The solution of inequality (15) gives the condition $ka > 0.5$.

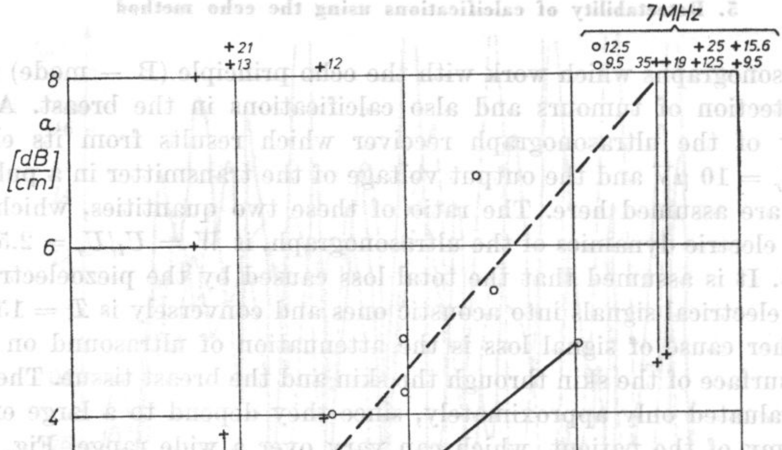

Fig. 8. Attenuation in the tissue of normal (points) and pathological (crosses) breasts, measured by different authors [8, 9]. The solid lines represent the measured value ranges given by the authors. (The values beyond the range of the diagram are given at the points and crosses). The dashed line represents the value of attenuation assumed in the present calcifications

When an elastic sphere is assumed as the calcification model, from formula (9),

$$\frac{p_s}{p_0} = \frac{ka}{2kr} f_\infty(ka) > 10^{-4}. \tag{16}$$

The value of the function $f_\infty(ka)$ can be read from Figs. 5 and 6. Inequality (16) is then satisfied for $ka > 0.65$; the effect of the Poisson's ratio ν can be neglected.

It follows that the two calcification models, the rigid and elastic spheres give a similar value of ka, satisfying inequality (15) or, alternatively, (16).

Assumption of $ka = 0.65$, at a frequency of 3 MHz, gives the radius of the sphere $a = 52$ μm. This sphere gives a signal received by the ultrasonograph; one, however, which is close to its electronic noise level.

For $ka > 3$, from Fig. 7, the function $f_\infty(ka)$ can, according to the conclusions in chapter 4, be assumed to have a value of about one.

Table 1 shows the results of calcifications of the expected radius of the calcification which gives a signal at the level of electronic noise of the ultrasonograph, depending on the depth at which the calcification occurs. Over the range of low values of ka, $ka < 0.65$, the assumption as the calcification model of an elastic sphere (formula (16)) or a rigid, stationary one (formula (15)) gives small differences; in the case of the rigid, stationary sphere model the sphere radii calculated are about 20 per cent smaller. The dependence of the smallest sphere radius on the depth at which the calcification occurs is striking; at depths of 8 and 1 cm these radii are different by an order of magnitude (Fig. 9).

Table 1. The expected radius of a sphere-shaped calcification which gives an electric signal on the electronic noise level, calculated as a function of the depth R at which the calcification occurs, at a frequency of 3 MHz

R	[cm]	1	2	4	6	8
A	[dB]	7	13	26	40	53
$-(W-T-A)$	[dB]	−126	−120	−107	−93	−80
$-(W-T-A)$	(lin)	5×10^{-7}	10^{-6}	4.5×10^{-6}	2.2×10^{-5}	10^{-4}
ka from (16)		0.05	0.08	0.17	0.34	0.65
ka from (15)		0.042	0.067	0.14	0.27	0.50
a from (16)	[μm]	4.0	6.3	13	27	52
a from (15)	[μm]	3.3	5.3	11	21	48

It follows from the analysis performed so far that even microcalcifications give signals detected by the ultrasonograph. It does not signify, however, that such signals can be recognized among the many signals obtained at the boundaries of fat, fibre and gland tissues and their heterogeneities. Microphotographs of the milk gland show discrete structures in the form of polygons with diagonals from 50 μm to 200 μm [19]. A lack of information on the value of the scattering coefficient of ultrasound in so heterogeneous breast tissue prevents an evaluation of the tissue interference whose level is much higher than the electronic noise level of the ultrasonograph. The magnitude of the tissue interference signal can be determined experimentally.

6. Experimental investigation of the tissue interference

The experimental investigations were performed using an USK 79/M ultrasonocardiograph, developed at the Department of Ultrasound, Institute of Fundamental Research [6], at a frequency of 3 MHz. This device is equipped with a piezoelectric transducer of 15 mm diameter with a plastic lens which focuses an ultrasonic beam at a distance of 6 cm from the surface of the transducer. At this distance the width of the ultrasonic beam, measured between -20 dB levels with respect to the maximum, is 9 mm. The piezoelectric transducer swings over an angle of 30°, thus exploring the area of the body under examination at a frequency of about 25 swings per second.

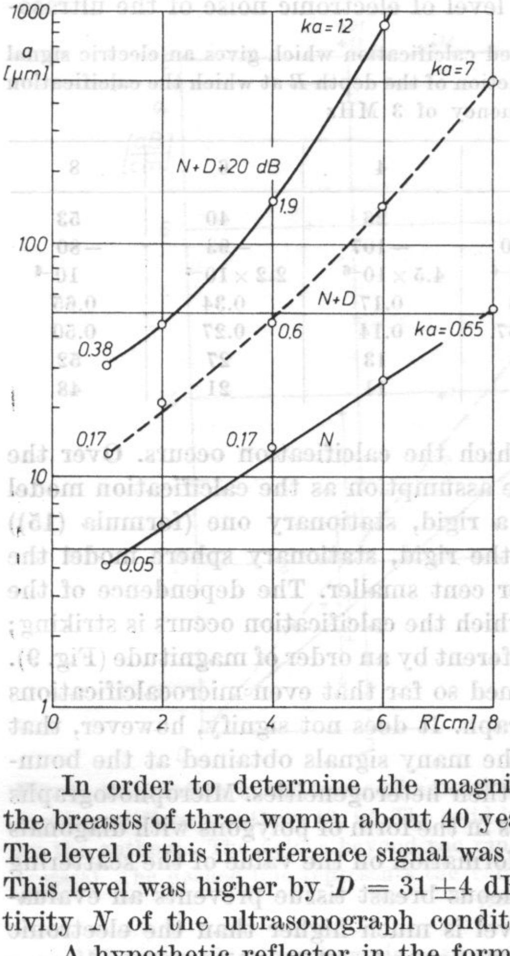

Fig. 9. The expected dependence of the detectability of calcifications on the depth at which they occur in the breast tissue, with the echo method at a frequency of 3 MHz. a – radius of the smallest detectable calcification which gives an electric signal on the electronic noise level (N), on the level of the tissue interference signals ($N+D$) and on a level higher by 20 dB than the tissue interference ($N+D+20$ dB), R – depth at which the calcification occurs. The respective values of ka are given at the points

In order to determine the magnitude of the tissue interference signal, the breasts of three women about 40 years old were examined using this device. The level of this interference signal was determined at a depth of 4 cm (Fig. 10). This level was higher by $D = 31 \pm 4$ dB than the level of the maximum sensitivity N of the ultrasonograph conditioned by the electronic noise.

A hypothetic reflector in the form of a half-space with the characteristic acoustic impedance $\varrho' c'$ can now be introduced. It can be assumed that the tissue interference results from the reflection of a plane wave incident perpendicularly at a flat surface limiting the present hypothetic reflector. The flat surface of the reflector is at the distance $R = 4$ cm from the surface of the probe, i.e. at the same distance at which the tissue interference signal in the women's breasts was measured.

The level of the amplitude of the wave incident on the surface of the hypothetic reflector is, with respect to the level of the electric signal of the transmitter (Fig. 10),

$$-T/2-A/2 \quad [\mathrm{dB}]. \tag{17}$$

Simplifying the problem, one can neglect the focusing of the ultrasonic beam, which in the present case is small, in view of the low ratio of the diameter of the transducer to the focal length, i.e. 0.25.

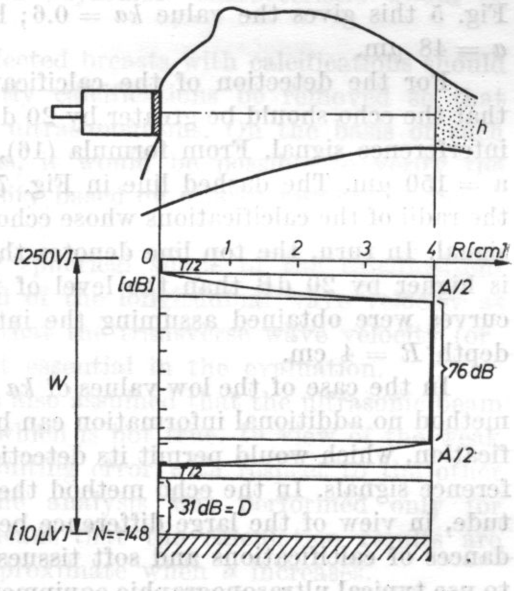

Fig. 10. The signal level as a function of the distance R in the determination of the tissue interference in the breast. 0 – level of the electric signal transmitted, T – electroacoustic transducing loss, A – wave attenuation loss, N – electronic noise level, D – experimentally determined increase in the level caused by the tissue interference signals, W – electrical dynamics of the ultrasonograph, h – hypothetic tissue reflector

The level of the amplitude of the wave reflected from the reflector is

$$N+D+T/2+A/2 \quad [\mathrm{dB}]. \tag{18}$$

The difference between levels (18) and (17) corresponds to the amplitude ratio of the reflected wave to the one incident on the surface of the reflector. Consideration of the values $N = 148$ dB, $D = 31$ dB, $T = 15$ dB and $A = 26$ dB gives

$$N+D+T+A = -76 \text{ dB} = 1.6\times 10^{-4} = \frac{\varrho c - \varrho' c'}{\varrho c + \varrho' c'} \cong \frac{\Delta \varrho c}{2\varrho c}. \tag{19}$$

In expression (19) the amplitude ratio of these waves is equated to the reflection coefficient of the plane wave at the interface between the tissue medium and the hypothetic reflector. The tissue medium would then show very small changes in the acoustic impedance $\Delta\varrho c/\varrho c = 3.2\times 10^{-4}$, which cause the tissue interference.

The present considerations were reduced to the equivalent (hypothetic) flat reflector. In reality the dimensions of the interfering tissue heterogeneities are comparable to the wavelength and, therefore, the scattering of the detected wave can be assumed and the amplitude of this wave decreases with increasing distance. Real, local differences in the acoustic impedance of the tissue medium can then be greater by an order of magnitude than the value of (19).

On the basis of the value of relation (19), from formula (16), it is possible to determine the product ka of a sphere-shaped calcification which gives an echo at the level of the tissue interference signal. For the value of $f_\infty(ka)$ in Fig. 5 this gives the value $ka = 0.6$; hence, the radius of the calcification is $a = 48$ μm.

For the detection of the calcification to be certain, it can be assumed that the echo should be greater by 20 dB (10 times) than the level of the tissue interference signal. From formula (16), in this case $ka = 1.9$ and accordingly $a = 150$ μm. The dashed line in Fig. 7 represents as a function of the depth the radii of the calcifications whose echo is at the level of the tissue interference signal. In turn, the top line denotes the radii of the calcifications whose echo is higher by 20 dB than the level of the tissue interference signal. The two curves were obtained assuming the interference signal level measured at the depth $R = 4$ cm.

In the case of the low values of ka for calcifications detected by the echo method no additional information can be obtained, e.g. on the shape of a calcification, which would permit its detection from the background of tissue interference signals. In the echo method the only discriminator is the signal amplitude, in view of the large difference between the characteristic acoustic impedances of calcifications and soft tissues. It is therefore ill-advised in this case to use typical ultrasonographic equipment with a receiver of logarithmic characteristic, which introduces a compression of echoes detected. The receiver should show a linear relationship between the output and input voltages.

7. Conclusions

It was shown that in the echo method using a typical ultrasonograph at a frequency of 3 MHz sphere-shaped calcifications with radii from 4 μm to 52 μm, depending on the depth at which they occur, give signals at the electronic noise level.

The detectability by the echo method is restricted by breast tissue heterogeneities which constitute the background of the tissue interference signals. The level of these interference signals was determined by examinations of normal breasts in 3 women about 40 years old, at a depth of 4 cm. From these results, the radii of the calcifications were determined which give a signal level 20 dB higher than the level of the tissue interference signals. These radii are 0.05; 0.15 and 1 mm at the respective depths of 2, 4 and 6 cm (Fig. 9). Their dependence on the depth results mainly from the attenuation loss in the tissue which in turn depends on the path of ultrasonic waves.

In the examinations by the echo method it is desired that a receiver with a linear relationship between the output and input signals should be used, since the use of logarithmic receivers causes signals to be compressed. This results in the loss of information on the signal amplitude which distinguishes the echo from a calcification from the echoes constituting the tissue interference background signals. A receiver with an adjustable characteristic would be the best.

It is recommended that tumour-affected breasts with calcifications should be examined clinically and subsequently calcifications be removed so that their size may be correlated with the ultrasonograms. On the basis of such clinical and experimental investigations, it would be possible to verify the present conclusions, which are of neccesity based on a large number of approximations.

These approximations include the spherical shape of the calcifications and the same values of its density and of the longitudinal wave velocity as those of the skull bone. It was shown that the transverse wave velocity (or the value of the Poisson's ratio) is not essential in the evaluation.

In the present considerations it was also assumed that the ultrasonic beam is a parallel homogeneous plane wave, which is not true. In view of the weak focusing of the beam, however, the resulting error with respect to the other approximations can be neglected. The analysis was performed only for steady-state (continuous wave). This means that the calculation results are exact for small radii *a* and become approximate when *a* increases.

Acknowledgement. The author is grateful to Dr. G. Łypacewicz for her measurements in breasts and to Dr. T. Kujawska for her elaboration of computer programs.

References

[1] R. C. Chivers, L. W. Anson, *Calculations of the backscattering and radiation force functions of spherical targets for use in ultrasonic beam assessment*, Ultrasonics, **20**, 1, 1, 25-34 (1982).

[2] L. Dragonette, M. Vogt, L. Flax, W. Neubauer, *Acoustic reflection from elastic spheres* II. *Transient analysis*, J. Acoust. Soc. Am., **55**, 1130-1137 (1974).

[3] J. Faran, *Sound scattering by solid cylinders and spheres*, J. Acoust. Soc. Am., **23**, 4, 405-418 (1951).

[4] L. Filipczyński, I. Roszkowski (eds), *Ultrasonic diagnosis in obstetrics and gynaecology* (in Polish), PZWL, Warsaw 1977.

[5] L. Filipczyński, *Detectability of gas bubbles in blood by the ultrasonic method*, Archives of Acoustics (in press).

[6] L. Filipczyński, J. Sałkowski, *Attempts at the ultrasonic visualization of the heart in real time*, Archives of Acoustics, **2**, 225-230 (1977).

[7] L. Flax, C. R. Dragonette, H. Uberall, *Theory of elastic resonance excitation by sound scattering*, J. Acoust. Soc. Am., **63**, 3, 723-731 (1978).

[8] S. Goss, E. Johnston, F. Dunn, *Comprehensive compilation of empirical ultrasonic properties of mammalian tissues*, J. Acoust. Soc. Am., **64**, 2, 423-457 (1978).

[9] S. Goss, E. Johnston, F. Funn, *Compilation of empirical properties of mammalian tissues*. II, J. Acoust. Soc. Am., **68**, 1, 93-107 (1980).

[10] B. J. Hackeloer, B. Huneke, V. Duda, R. Eulenburg, G. Lauth, R. Buchholz, *Sonografische Differentialdiagnose der Mammakarzinome*, Ultraschall in der Medizine, **2**, 129-134 (1981).

[11] L. D. Hampton, C. M. McKiney, *Experimental study of the scattering of acoustic energy from solid metal spheres in water*, J. Acoust. Soc. Am., **33**, 5, 664-673 (1961).

[12] R. Hickling, *Analysis of echoes from a solid elastic sphere in water*, J. Acoust. Soc. Am., **34**, 1582-1592 (1962).

[13] R. Hickling, N. Wang, *Scattering of sound by a rigid movable sphere*, J. Acoust. Soc. Am., **39**, 276-279 (1966).

[14] C. R. Hill, V. R. McCready, D. O. Cergrove (eds.), *Ultrasound in tumor diagnosis*, Pitman Medical, Kent 1978.

[15] G. Łypacewicz, T. Powałowski, K. Łukawska, *Ultrasonic examination of breast tumors with Doppler method*, Proc. of the 2nd Congress of the Federation of Acoustical Societes of Europe, PAN, Warsaw, II, 153-156, 1978.

[16] V. Menges, *Mammographie, die zuverlässigste Ultersuchungsmethode zur Brustkrebs-Früherkennung*, Electromedica, **2**, 42-49 (1979).

[17] P. Morse, K. Ingard, *Theoretical acoustics*, McGraw Hill, New York 1968.

[18] W. Neubauer, M. Vogt, L. Dragonette, *Acoustic reflection from elastic spheres. I. Steady-state signals*, J. Acoust. Soc. Am., **55**, 1123-1129 (1974).

[19] T. Pawlikowski, M. Karasek, M. Pawlikowski, *Histology handbook* (in Polish), PZWZ, Warsaw 1981.

[20] S. N. Rshevkin, *Kurs leksij po teorii zvuka*, Moscow 1980.

[21] *Second International Congress on the Ultrasonic Examination of the Breast*, London June 22-23, 1981, Abstracts, Institute of Cancer Research.

[22] T. Hasegawa, K. Yosioka, *Acoustic radiation force on a solid elastic sphere*, J. Acoust. Soc. Am., **46**, 5 (P2), 1139-1143 (1969).

[23] D. N. White, G. R. Curry, R. J. Stevenson, *The acoustic characteristic of the scull*, Ultrasound in Medicine and Biology, **4**, 3, 225-252 (1978).

[24] Y. N. Chen, S. J. Kim, *Scattering of acoustic waves by a penetrable sphere with statistically corrugated surface*, J. Acoust. Soc. Am., **42**, 1-5 (1967).

Received on 25 January, 1983.